Head-Waves Parametric Rolling of Surface Combatant

Frederick Stern[1] and Emilio F. Campana[2]
[1] IIHR - Hydroscience & Engineering, The University of Iowa, Iowa City, IA, 52242, USA
[2] INSEAN - Italian Ship Model Basin, Via di Vallerano 139, 00128 Roma, Italy

Frederick-stern@uiowa.edu

ABSTRACT

Complementary CFD, towing tank EFD, and nonlinear dynamics approach study of parametric roll for the ONR Tumblehome surface combatant both with and without bilge keels is presented. The investigations without bilge keels include a wide range of conditions. CFD closely agrees with EFD for resistance, sinkage, and trim except for Fr>0.5 which may be due to free surface and/or turbulence modeling. CFD shows fairly close agreement with EFD for forward speed roll decay in calm water, although damping is over/under predicted for largest/smaller GM. Most importantly CFD shows remarkably close agreement with EFD for forward speed roll decay/parametric roll in head waves for GM=0.038 and 0.033 m, although CFD predicts larger instability zones at high and low Fr, respectively. Nonlinear dynamics approaches are in qualitative agreement with CFD and EFD. The CFD and nonlinear dynamics approach results were blind in that the correct EFD radius of gyration k_{xx} was not known a priori.

1.0 INTRODUCTION

Ships with pronounced bow flare, flat transom sterns, and wall-sided/wide-beam mid-ship sections are vulnerable to large amplitude roll limit-cycle oscillations suddenly occurring especially in head or stern seas, which is referred to as parametric roll. Causes in order of importance include periodic changes of transverse stability (restoring moment) from increased/decreased stability when ship encounters wave trough/crest, nonlinear restoring moment, and nonlinear roll-pitch-heave resonance. Large roll motions are major source of discomfort and limiting factors in the operability of ships and can lead to loss of life, damage and capsize. The probability of occurrence is exacerbated by the traditional maritime practice of steering into heavy-weather head seas at reduced speed, although recent international guidelines provide alternative recommendations.

Theoretical/analytical dynamics provides a mathematical framework and qualitative understanding. The roll motion neglecting nonlinear damping and restoring moment and considering wave effects and pitch-heave coupling only through a time varying restoring coefficient is modeled as a 1D mass-spring-damper linear system with periodic restoring coefficient and small damping, which can be transformed into the Mathieu equation. Bounded/unbounded solutions to the Mathieu equation are delineated in the Ince-Strutt diagram as $q = \omega_a^2 / \omega_e^2$ vs. $p = (\omega_\phi^2 - \alpha^2) / \omega_e^2$ curves where ω_ϕ is the roll natural frequency in waves, ω_a is the roll excitation frequency in waves, ω_e is the encounter frequency ($= \omega_w + 2\pi U / \lambda$, where $\omega_w = \sqrt{2\pi g / \lambda}$ and λ are the wave frequency and length and U is the ship speed), and α is the linear roll damping. Linear and higher-order theories for the first instability zone provide instability estimates for small q. For q=0.0, instability occurs at p=0.25 and for zero damping $\omega_e = 2\omega_\phi$: in other words for small excitation and damping the roll period equals twice the wave encounter/pitch motion period. For q>0.0 instability occurs for increasing ranges of p for increasing q, which can be equivalently expressed as a Froude number (Fr) range. Typically largest ship motions/roll excitation occurs for wavelengths about $\lambda / L \approx 1.33$ where L is

ship length. Unbounded solutions to the Mathieu equation may not lead to unbounded roll unless the damping α is less than a threshold value $\alpha_T=\alpha_T(p,q)$. More advanced theories include nonlinear damping and restoring and nonlinear roll-pitch-heave coupling mathematical models solved using computational dynamics methods. Both linear and more advanced approaches have been validated using towing tank tests. Implementing the Mathieu equation and more advanced approaches including 6DOF models for quantitative criteria and prediction of parametric roll requires estimates of ω_ϕ, ω_a, α for linear models and additionally nonlinear and coupling terms for nonlinear models. Simple hydrostatic and potential flow strip theories and 3D panel methods have been used for this purpose, but these approaches typically require empirical estimates or towing tank tests for linear α and nonlinear damping and other terms, which is a major limitation. URANS CFD codes for ship hydrodynamics offers possibility of providing a complete rational-mechanics based prediction capability of parametric roll for improved safety criteria and increased physical understanding.

The present paper describes a complementary CFD, towing tank EFD, and nonlinear dynamics approach study of parametric roll for the ONR Tumblehome (OT) surface combatant both with (preliminary CFD and EFD studies [1]) and without bilge keels. The investigations without bilge keels include a wide range of conditions: 2DOF heave-pitch resistance C_T, sinkage σ, and trim τ in calm water; 2DOF heave-roll forward speed roll decay in calm water for varying metacentric height GM; and 3DOF heave-roll-pitch forward speed roll decay/parametric roll in head waves for varying wave steepness Ak, GM, and drift angle. References [2,3,4] provide details of the EFD studies. The URANS code CFDSHIP-IOWA version 4.0 [5,6,7] is used. The CFD and EFD results are compared with Mathieu equation and nonlinear dynamics approach [8,9].

2.0 SHIP MODEL, TEST DESIGN, AND CONDITIONS

2.1 Ship Model and Test Design

Figure 1 shows the OT, which is preliminary design for a new concept surface combatant. Table 1 provides particulars of the CFD and EFD geometries and installation conditions. The scale ratio is 46.6. The EFD model was ballasted to achieve the specified displacement, longitudinal and vertical centers of gravity (LCG, KG) and radii of gyration (k_{xx}, k_{yy}) using the added ballast, pendulum, and inclining methods. Later revised estimates of radii of gyration were determined, as indicated Table 1. The primary purpose of the tests was to realize parametric roll under 3DOF semi-captive conditions (constrained in surge, sway, and yaw and free to heave, roll, and pitch) by releasing the model towed at constant Fr at an initial roll angle ϕ_0 in head waves with $\lambda/L=1$ and varying Fr to determine the instability zone. The wave signal was used to control the release of the model such that a wave crest was located at mid ships when the just released model has zero roll angle.

2.2 Preliminary Studies

Preliminary studies were conducted with bilge keels to investigate large amplitude roll (beam waves), parametric roll (head waves) and pure loss of stability (following waves). 2DOF zero-speed heave-roll in beam waves was investigated for $\lambda/L=1.12$, i.e. wave frequency equal natural frequency roll, and wave steepness Ak=(0.034,.073,0.156,0.203) for EFD and Ak=0.156 for CFD. The roll natural frequency f_ϕ=0.65 Hz was based on the Ak=0.034 tests, which is close to the hydrostatic estimate $f_{\phi h}$=0.68. 3DOF forward-speed heave-roll-pitch in head waves was investigated for $\lambda/L=1$, i.e. f_w=0.69 Hz and Fr=.35 such that encounter frequency $f_e=2f_\phi$=1.297, Ak=(0.073,0.115,0.156) for EFD and Ak=(0.115,0.156) for CFD, and ϕ_0=(10,20,30) deg for EFD and ϕ_0=30 deg for CFD. This condition corresponds to the linear

theory instability estimate for small excitation and zero damping. 3DOF forward-speed heave-roll-pitch in following waves was investigated for $\lambda/L=1$, i.e. f_w=0.69 Hz and Fr=.4 such that encounter frequency f_e=0.0, Ak=0.156, and model released with an initial roll angle ϕ_0 with wave crests near mid ship and bow/stern. CFD was not performed.

Table 2 summarizes the 2DOF zero-speed heave-roll in beam waves results for Ak=0.156. EFD indicates dominant first harmonic for heave, roll, side force, and yaw moment, whereas surge force and pitch moment are dominant second harmonic. Heave and roll amplitudes are large, i.e., greater that A and Ak, respectively. Surge force third and fourth harmonics are nearly as large as the first and second, respectively. Dominant second harmonic for pitch moment is expected due to fore and aft body asymmetry, which induces dominant second harmonic for surge force. Overall results indicate heave-roll motions induce large surge force and pitch and yaw moments. Heave and roll amplitudes increase linearly with A and Ak, respectively. CFD qualitatively predicts these trends. Heave and yaw moment are over predicted, whereas roll, surge and side force, and pitch moment are under predicted. The largest errors are for roll, surge force, and pitch moment. The phase for the dominant harmonic is fairly well predicted for heave, roll, and side force, but the differences are larger for surge force and yaw and pitch moments. CFD analysis shows that dominant second harmonic for pitch moment results from equal contributions from hydrostatic and pressure components, which are larger than friction component and 180 deg out of phase.

Table 3 summarizes the 3DOF forward-speed heave-roll-pitch in head waves results for Ak=.115 and .156 (CFD only) and ϕ_0=30 deg. EFD indicates dominant first harmonic response for heave, pitch, and surge force X, whereas roll, side force Y, and yaw moment N are damped harmonic oscillations, i.e., parametric roll is not exhibited. Surge force second harmonic amplitude is fairly large. Roll decay first peak, linear and nonlinear damping, and large/small mean roll angle frequency are $.4\phi_0$, .55 and .0052, and $.91f_{\phi h}/f_e$, respectively. The linear damping corresponds to a logarithmic decrement $\delta=\ln(\phi_i/\phi_{i+1})$ of .82 and energy ratio $e^{2\delta}$ of 5.2. Overall results indicate heave-roll-pitch motions induce large surge and sway forces and yaw moment. CFD qualitatively predicts these trends. Heave and pitch amplitude and phase as well as surge force phase are close to EFD, whereas as surge force amplitude is under predicted. Roll decay first peak, linear and nonlinear damping, and large/small mean roll angle frequency are $.5\phi_0$, .4 and .0061, and $.89f_{\phi h}/f_e$, respectively, which are close to EFD. CFD shows that increased Ak reduces z/A, θ/Ak, and ϕ/Ak, but increases surge force amplitude and roll, side force, and yaw moment decay. Roll decay first peak, linear and nonlinear damping, and large/small mean roll angle frequency are $.33\phi_0$, .68 and .0089, and $.74f_{\phi h}/f_e$, respectively. CFD analysis of roll moment and GM variation for Ak=.115, provides the mean $GM_m=(GM_{max}+GM_{min})/2$=0.033 (note that GM=0.043 m) and excitation $GM_a=(GM_{max}-GM_{min})/2$=0.021 from which $\omega_\phi=\sqrt{gGM_m}/k_{xx}$=3.71 (note that $\omega_{\phi h}=\sqrt{gGM}/k_{xx}$=4.24 rad/s) and $\omega_a=\sqrt{gGM_a}/k_{xx}$=2.89 rad/s such that (p,q)= (0.2, 0.12) with instability range 0.17<Fr<0.38 and α_T=0.32. However, $\alpha=0.4>\alpha_T$ which is explanation for with bilge keels study not achieving parametric roll.

The 3DOF following wave EFD did not indicate loss of stability, but rather highly damped roll oscillations. The roll logarithmic decrements, energy ratios, and frequencies were 3.50 and 1.30, 1141 and 14, and $.92f_{\phi h}$ and $.53f_{\phi h}$, respectively, for mid ship and bow/stern. The mid ship condition was susceptible to bow diving.

2.3 Without Bilge Keels Conditions

First CFD was conducted for forward speed roll decay/parametric roll in head waves for $\lambda/L=1$,

$0.0 \le Fr \le 0.44$, and different GM with k_{xx}=0.153 m and Ak=0.115. For GM=0.043 sensitivity studies were conducted for larger Ak=0.156 for Fr=0.13, 0.15, and 0.2 and for drift angle β=2 and 4 deg for Fr=0.13 with Ak=0.115. Second EFD was conducted for resistance in calm water C_T, σ, and τ for $0.05 \le Fr \le 0.45$; forward speed roll decay in calm water for $0.05 \le Fr \le 0.35$ and ϕ_0=30 deg (GM=.033 m), $0.05 \le Fr \le 0.35$ and ϕ_0=30 deg (GM=.038 m), and $0.05 \le Fr \le 0.45$ and ϕ_0=25 deg (GM=.043 m); and forward speed roll decay/parametric roll in head waves for $\lambda / L = 1$, $0.02 \le Fr \le 0.44$, ϕ_0=25 deg, and different GM and Ak. Third CFD was conducted for C_T, σ, and τ for $0.0 \le Fr \le 0.6$; forward speed roll decay in calm water for Fr=0.2 and ϕ_0=30 deg (GM=.033 m), Fr=0.05, 0.2, and 0.35 and ϕ_0=30 deg (GM=.038 m), and Fr=0.2 and ϕ_0=25 deg (GM=.043 m) and different k_{xx}; and forward speed roll decay/parametric roll in head waves for $\lambda / L = 1$, $0.02 \le Fr \le 0.44$, ϕ_0=30 deg and different GM, k_{xx}, and Ak. Fourth, nonlinear dynamics approach was implemented. Fifth and lastly, additional EFD radii of gyration tests were conducted.

3.0 CFD METHODS

CFDSHIP-IOWA is a general purpose URANS/DES solver developed at IIHR over the last 15 years for ship hydrodynamics applications. Either absolute or relative inertial non-orthogonal curvilinear coordinate system for arbitrary moving but non-deforming control volumes and solutions domains is used. Turbulence models include isotropic, non-isotropic, and DES with near-wall or wall functions. Single- and two-phase level set methods are used for free-surface and interface capturing, respectively. Captive, semi-captive, and full 6DOF motions/forces/moments are simulated for multi-objects with parent/child hierarchy. Numerical methods include advanced iterative solvers, 2nd and higher order finite difference with conservative formulation, PISO or projection method solution of pressure Poisson equation, and HPC with MPI-based domain decomposition. Block structured dynamic overset grids using SUGGAR [10]. Forces and moments computed in overlap regions using USURP [11].

Relative inertial coordinates were used for beam and head wave cases and absolute inertial coordinates were used for resistance. The k-ω with near wall turbulence model was used. 3-5 inner iterations were used for convergence of the flow field equations within each time step. Convergence of the pressure equation is reached when the residual imbalance of the Poisson equation drops six orders of magnitude. All other variables are assumed converged when the residuals drop to 10^{-5}. The computational domains extend from $-0.5 < x < 2, -1 < y < 1, -1 < z < 0.25$ for the head wave cases and resistance test and $-1 < x < 2$, $-1 < y < 2.25$, $-1 < z < 0.25$ for beam wave cases, in dimensionless coordinates based on L. The ship axis is aligned with the x-axis with the bow at x = 0 and the stern at x = 1. The free surface at rest lies at z = 0. The initial conditions are the corresponding beam or head waves for each case. At t = 0, the ship is accelerated impulsively to full speed for beam and head waves while ship is accelerated very slowly to determine resistance, sinkage, and trim at different Fr numbers in calm water. Computational grids for the hull and bilge keels are designed to accurately resolve geometric features of the model and the unsteady turbulent boundary layer, wake, and wave fields. The hull boundary layer and bilge keels grids were generated using GRIDGEN. The hull boundary layer and bilge keels grid were fixed to and move with the ship. The hull boundary layer has a double-O topology and was created with a hyperbolic grid generator, with a grid spacing at the hull designed to yield y^+ <1 for the highest Reynolds number case Fr = 0.6. In this way the same boundary layer grid could be used for all cases. The hull boundary layer grid extends to cover the deck of the ship and wraps around it, allowing for computations with extreme motions. Grid topology was selected so that two other blocks were responsible to capture the flow near the hull (refinement block) and far from the hull (background block). Since there is a wave on the free surface, the background block was designed to have enough grid points near free surface. The computational domain for all blocks covers both the port and starboard sides of the ship, since the flow and wave fields are asymmetric during the roll motion. For the grid convergence study, a fine grid 11M and a coarse grid

1.4M were generated by refining and coarsening the medium grid 4M using a factor of $\sqrt{2}$ in each direction with a tri-linear interpolation algorithm, so that the grid distribution and shape would be as close as possible to the original grid. This grid study was performed for the ship with 10 deg heel angle towed in calm water, free to sink and trim, and for all Fr numbers in the range of 0-0.6. Figure 2 shows the grid for ship and the solution domain.

4.0 EFD METHODS

The tests were conducted in the INSEAN 220x9x3.5 m towing tank with a flap type wave maker. The model is made from fibreglass. Model motions are measured using both an optical motion tracker and gyroscopic platform. A custom designed load cell and mount located at the model center of gravity was used for the force and moment measurements, which also allowed the required DOF. A servo-mechanism wave gauge was used for the wave elevation measurements. Uncertainty analysis was conducted for GM=.038 m, Ak=0.115, and Fr=0.2 following standard procedures including five repeat tests.

5.0 NONLINEAR DYNAMICS APPROACH

An uncoupled 1DOF nonlinear roll mathematical model is used:

$$\ddot{\phi} + 2\alpha\dot{\phi} + \gamma\dot{\phi}^3 + \omega_\phi^2\phi + \omega_\phi^2 l_3\phi^3 + \omega_\phi^2 l_5\phi^5 + \omega_\phi^2\{GM_m + GM_a\cos\omega_e t\}\phi / GM = 0 \quad (1)$$

Linear and cubic roll damping coefficients are estimated from towing tank forward speed roll decay test using Himeno method [12], as a function of Fr. The quadratic roll damping term $\beta|\dot{\phi}|\dot{\phi}$ was neglected since it makes analysis more difficult and has been shown to have small affects on predictions, as long as cubic roll damping term is included. Metacentric height variation GM_a and GM_m are estimated from towing tank tests conducted at Osaka University for model with bilge keels for 2DOF forward speed heave-pitch in head waves with 10 degree heel angle at several Fr and GM=0.038 m. k_{xx}=0.1388 m was estimated by adjusting ω_ϕ for best fit to Fr=0.05 and GM=0.038 m roll decay test data and assuming $\omega_\phi = \omega_{\phi h} = \sqrt{gGM} / k_{xx}$ =4.39 rad/s. Nonlinear restoring coefficients are estimated from odd cubic polynomial best fit to Fr=0.0 roll moment towing tank test data for $2 \le \phi \le 20$ deg. Parametric roll is strongly nonlinear such that multiple stable solutions could coexist because of dependency on initial conditions. Time domain simulations could fail to reveal all possible danger of parametric roll. Therefore, Poincaré mapping and averaging methods are used as geometrical and analytical approaches within the framework of nonlinear dynamics.

Poincaré mapping was applied to identify steady states of parametric roll as a function of Fr by integrating Eq. (1) using Runge-Kutta method. Once a steady state for certain Fr is found, the next numerical integration of Eq. (1) starts from the obtained steady state but with a slightly different Fr, e.g. 0.001. First 100 cycles are ignored as a transient state, and the roll angle as the Poincaré map for the next 50 cycles are plotted. Here the Poincaré section is set to the instant when the model center of gravity is passing by a wave trough because maximum parametric roll amplitude in head waves appears around wave trough. In case roll motion completely damps within 100 cycles, the initial roll angle for next Fr is reset to initial value of 0.1 degrees. Both tracing directions of increasing and decreasing Fr were explored to demonstrate dependency of initial condition.

The Poincaré map is useful to identify bifurcation structures of roll motion, but it requires an initial steady state for continuously tracing steady states. Thus there is still the possibility that another stable state exists with the same condition. In addition, numerical simulations for all possible condition parameters, wave

height, wave length, ship speed, GM, etc. consume tremendous simulation time. Therefore, an averaging method was used, which is one of the analytical approaches in nonlinear dynamics for solving Eq. (1). Here all steady states of principal parametric roll, where roll frequency is a half of the encounter frequency, can be theoretically determined because steady states are solutions of algebraic equations.

$$A = 0 \tag{2}$$

$$\{\alpha + \frac{3}{8}\gamma\bar{\omega}^2 A^2\}^2 + \{\frac{\bar{\omega}}{2} - \frac{1}{2}\frac{\omega_\phi^2}{\bar{\omega}}(1 + GM_{mean}/GM + \frac{3}{4}l_3 A^2 + \frac{5}{8}l_5 A^4)\}^2 = (GM_{amp}\frac{\omega_\phi^2}{4\bar{\omega}}/GM)^2 \tag{3}$$

Eq.(2) indicates a trivial solution at 0 degrees of roll. Steady states of the parametric rolling orbit can be obtained by solving the above eighth-degree algebraic equation. If locally these equations are linearized at their steady states, stability of solutions can be examined with their eigenvalues, and their attractor domain can be determined with their eigenvectors.

6.0 COMPARISON CFD, EFD, AND NONLINEAR DYNAMICS METHODS

6.1 Resistance, Sinkage, and Trim

Figure 3 compares EFD and CFD for C_T, σ, and τ, including with and without bilge keels. In general the results indicate expected trends and excellent agreement CFD and EFD (average error $E_{CT,\sigma,\tau}$ =1.5, 5.02, 2.13 %D), except for σ for $0.45 \le Fr \le 0.55$ and for τ for Fr>.55 for which CFD under predicts EFD by maximum $E_{CT,\sigma,\tau}$ =4.11 17.7, 6.43 %D. Single Fr=0.5 CFD shows same values as full curve CFD at same Fr. A CFD grid study for forward speed, calm water, 10 deg heel angle, and free to sink and trim for all Fr numbers in the range of 0-0.6 indicates relatively small dependency on grids, which suggests large Fr errors are due to either free surface and/or turbulence modeling.

6.2 Forward Speed Roll Decay in Calm Water

For GM=0.038 m and Fr=0.2, CFD roll with k_{xx}=0.146 m show large differences EFD roll with average absolute value error E=380%ϕ_0, i.e. CFD under/over predicts large roll angle damping/period. k_{xx}=0.146 m was improved EFD estimate for without bilge keels conditions. CFD with reduced k_{xx}=0.1246 m indicates much closer agreement EFD, at least for large roll angles, although damping is still under predicted with E=5%ϕ_0. The under prediction is larger for Fr=0.05 and 0.35 with E=9.3 and 12.7%ϕ_o. Similarly for GM=0.033 and 0.043 m and Fr=0.2 reduced values of k_{xx}=0.1388 and 0.1298 m indicate closer agreement EFD, although damping is under and over predicted with E=14 and 8%ϕ_0. Figure 4b compares CFD and EFD for GM=0.043 m and Fr=.2.

Figure 5 compares CFD and EFD non-dimensional linear and nonlinear damping coefficients based on Himeno method (α,γ,α_e) and linear damping coefficient based on $n\omega_{\phi d}$ where n=δ/2π and damped roll period $\omega_{\phi d}$ are averaged over all mean roll angles $\phi_m = (\phi_{j-1} + \phi_j)/2$. Dimensional linear damping increases with Fr^n with n<1; thus, non-dimensional linear damping decreases with Fr^{1-n}. For EFD equivalent linear damping α_e n=.48, .36, and .35 for GM=0.033, 0.038, and 0.043 m with similar values for α and $n\omega_{\phi d}$; and linear damping increases for decreasing GM. CFD shows similar values linear damping for GM=0.043 m, but under predicts for lower GM. For both EFD and CFD nonlinear damping increases with Fr. CFD over predicts for GM=0.043 and under predicts for lower GM, especially GM=0.038 m and Fr=0.35. Figure 5 results are consistent with aforementioned CFD roll E, as shown in Fig. 4b. Equation (1) was integrated with EFD linear and nonlinear damping coefficients along with nonlinear restoring coefficients (Fig. 6a) and GM_a=GM_m=0 to assess the accuracy of the reconstructions. The best results are for nonlinear damping and restoring with E=10, 9, 6%ϕ_o for GM=0.043, 0.038, and 0.033 m, respectively,

averaged over Fr. Use of linear restoring increased E=21, 19, and 15%ϕ_o. Use of only the linear damping and nonlinear restoring coefficients increased E by only about 1%ϕ_o. Added mass is shown in Fig. 6b.

Lastly, OT forward speed roll decay is compared with EFD data for DTMB 5415 [13], i.e., previous generation surface combatant, as also shown in Fig. 4-6. Average roll angle is .3ϕ_o for 5415 vs. .1ϕ_o for OT. Non-dimensional linear damping is nearly constant for 5415 vs. Fr and smaller than OT for low Fr. Reconstructions show that for 5415 the best results for α_e with E=11%ϕ_o without requiring nonlinear restoring coefficient. In conclusion, best reconstruction for OT requires nonlinear damping and restoring coefficients with n<1 for current Fr range and E about 10%ϕ_0, whereas for 5415 best reconstruction for equivalent linear damping without requiring nonlinear restoring coefficients with n about 1 and E about 11%ϕ_0. E values are similar to those for CFD.

6.3 Forward Speed Roll Decay/Parametric Roll in Head Waves

First CFD for GM=0.043, 0.038, and 0.048 m and k_{xx}=0.153 m (i.e., same value as for with bilge keels conditions), including for GM=0.043 m effects of Ak and β. Figure 7a shows the GM=0.043 m results. Parametric roll is predicted for $0.11 \le Fr \le 0.35$ with maximum stabilized roll angle $\phi_{\max} \approx 40$ deg for Fr=0.13. Increased wave steepness increases pitch amplitude, but inhibits parametric roll. Drift angle β=2 deg increases $\phi_{\max} \approx 43$, whereas β=4 deg inhibits parametric roll. For smaller GM=0.038 m capsize is predicted, whereas for larger GM=0.048 parametric roll is predicted for $0.11 \le Fr \le 0.35$ with maximum stabilized roll angle $\phi_{\max} \approx 60$ deg for Fr=0.18, as shown in Fig. 7c.

Second EFD for GM=0.043, 0.038, and 0.033 m with Ak=0.115, including for GM=0.038 effects Ak. For GM=0.043 m parametric roll is not shown, whereas for GM=0.038 parametric roll is shown for $0.18 \le Fr \le 0.35$ with maximum stabilized roll angle $\phi_{\max} \approx 35$ deg for Fr=0.18, as shown in Fig. 7b, and for GM=0.033 parametric roll indicated for $0.07 \le Fr \le 0.28$ with maximum stabilized roll angle $\phi_{\max} \approx 40$ deg for Fr=0.07, as shown in Fig. 7d. For GM=038 and smaller Ak=0.105 parametric roll indicated for $0.19 \le Fr \le 0.28$ with maximum stabilized roll angle $\phi_{\max} \approx 33.5$ deg for Fr=0.2, as shown in Fig. 7b.

Third CFD for GM=0.043, 0.038, and 0.033 m and k_{xx}=0.1298, 0.1246, and 0.1388 m, respectively, as estimated from the roll decay tests with Ak=0.115. For GM=0.043 m parametric roll is not shown, whereas for GM=0.038 m parametric roll is shown for $0.17 \le Fr \le 0.44$ with maximum stabilized roll angle $\phi_{\max} \approx 45$ deg for Fr=0.17, as shown in Fig. 7b, and for GM=0.033 m parametric roll indicated for $0.0 \le Fr \le 0.3$ with maximum stabilized roll angle $\phi_{\max} \approx 50$ deg for Fr=0.02, as shown in Fig. 7d. For GM=0.033 m and Fr=0 capsize is predicted. The agreement between CFD and EFD for GM=0.038 and 0.033 m is remarkable, although CFD predicts larger instability zones at high and low Fr, respectively. Figure 8 compares EFD and CFD parametric roll for GM=0.038 m and Fr=0.2, including motion and X,Y,N time histories and in latter case FFT.

Fourth, nonlinear dynamics approaches were implemented, as also shown on Fig. 7a,b,d. For GM=0.038 m, Poincaré mapping parametric roll appears at Fr=0.195 and disappears at Fr=0.38 in increasing direction, but it appears at 0.13 and disappear at 0.38 in decreasing direction. There is significant difference of roll angle from 0.13 to 0.195 in Fr, and this difference can be explained as a sub-critical bifurcation. This result indicates that initial value dependency of parametric roll of OT is significant and its steady state in sub-critical bifurcation region depends on initial condition significantly. The maximum stabilized roll angle is $\phi_{\max} \approx 30$ deg for Fr=0.2. Calculated region of parametric roll does not agree with

EFD result perfectly. This might be because restoring variation is expressed as GM variation in Eq. (1) by assuming restoring variation is linear to roll angle while roll angle of parametric roll is extremely large because of the lack of bilge keel. In addition, effect of water on deck has to be accurately taken into account particularly in high Fr for quantitative prediction. Averaging method agreement of roll amplitude in comparison with EFD result is not bad but stability of solutions is not so from 0.19 to 0.28 in Fr. This result may indicate that observed parametric roll in this region is not so stable that it could disappear if some external disturbance is given. Note that averaging method unstable solution means no parametric roll is observed in actuality. The maximum stabilized roll angle $\phi_{\max} \approx 28$ deg for Fr=0.28. For GM=0.033 m, Poincaré mapping parametric roll is indicated for $0.11 \le Fr \le 0.34$ with maximum stabilized roll angle $\phi_{\max} \approx 20$ deg for Fr=0.2 with no sub-critical bifurcation region and Averaging method parametric roll is indicated for $0.225 \le Fr \le 0.34$ with maximum stabilized roll angle $\phi_{\max} \approx 22.5$ deg for Fr=0.225, as shown in Fig. 7d. For GM=0.043 m, Poincaré mapping parametric roll is not indicated and Averaging method parametric roll is indicated for $0.325 \le Fr \le 0.35$ with maximum stabilized roll angle $\phi_{\max} \approx 29$ deg for Fr=0.325, as shown in Fig. 7a.

Fifth and lastly, additional EFD conducted for revised estimates k_{xx}=0.123, 0.125, and 0.127 m, respectively, for GM=0.043, 0.038, and 0.033 m and k_{yy}=0.737 m. The average k_{xx} difference between EFD and CFD is 5%. The EFD uncertainty in k_{xx} and GM are estimated at 2.5% and 2%, respectively. Tables 4 and 5 summarize and compare Mathieu equation and CFD and EFD estimates for mean and excitation GM and frequencies and the instability ranges and stabilized roll angles from EFD, CFD, nonlinear dynamics approach. The former are based on CFD and EFD for 2DOF forward speed heave-pitch in head waves with fixed heel angle. For EFD, ϕ_0=10 deg, GM=0.043, 0.038, and 0.033 m and Fr=0.1, 0.2 and 0.3 and for CFD, ϕ_0=30 deg, GM=0.043, 0.038, and 0.033 m, Fr=0.2, and Ak=0.115.

7.0 CONCLUSIONS

Complementary CFD, towing tank EFD, and nonlinear dynamics approach study of parametric roll for the OT surface combatant both with and without bilge keels is presented. The investigations without bilge keels include a wide range of conditions: 2DOF resistance C_T, sinkage σ, and trim τ in calm water; 2DOF forward speed roll decay in calm water for varying GM; and 3DOF forward speed roll decay/parametric roll in head waves for varying wave steepness Ak, GM, and drift angle. CFD closely agrees with EFD for resistance, sinkage, and trim, except for Fr>0.5, which may be due to free surface and/or turbulence modeling. CFD shows fairly close agreement with EFD for forward speed roll decay in calm water, although damping is over/under predicted for largest/smaller GM. Most importantly CFD shows remarkably close agreement with EFD for forward speed roll decay/parametric roll in head waves for GM=0.038 and 0.033 m, although CFD predicts larger instability zones at high and low Fr, respectively. Nonlinear dynamics approaches are in qualitative agreement with CFD and EFD. The CFD and nonlinear dynamics approach results were blind in that the correct EFD radius of gyration k_{xx} was not known a priori. Future work focuses on additional comparisons and evaluation of present study, including forward speed roll decay in waves vs. calm water, forward speed parametric roll motions, forces, and moment, and alternative 1DOF nonlinear dynamics approach with time dependent linear and nonlinear restoring terms [14]; and extension of EFD, CFD, and nonlinear dynamic approach for captive model static heel and drift in calm water and in the former case in head and following waves and free model broaching, surf riding, and periodic motion instability studies.

Acknowledgements

Seyed Hamid Sadat-Hosseini, IIHR, Angelo Olivieri, INSEAN, Alberto Francescutto, DINMA - Dept. of Naval, Architecture, Ocean and Environmental Eng., University of Trieste, Trieste, Italy, and Hirotada Hashimoto and Naoya Umeda, Dept. Naval Architecture & Ocean Engineering, Osaka University, Osaka, Japan, are co-authors. The Office of Naval Research under contract/grant N00014-01-1-0073, N00014-04-1-0288, and N00014-06-1-0646 for IIHR, INSEAN, and OU, respectively, administered by Dr. Patrick Purtell, sponsored this research. Partial support was provided by the Italian Minister of Transport for INSEAN and by Japan Society for Promotion of Science for OU. The CFD simulations were conduced utilizing DoD HPC. Dr. Il-Ryong Park performed the 2DOF beam wave CFD simulations. Dr. Arthur Reed provided many useful suggestions concerning the test design and evaluation of results.

References

1. Sadat-Hosseini, H., Park, I., Stern, F., Olivieri, A., Campana, E., Francescutto, A.," Complementary URANS CFD and EFD for Validation Extreme Motions Predictions," 9th ICNSH, Ann Arbor, MI, 5-8 August 2007.
2. Olivieri, A., Campana, E., Francescutto, A., and Stern, F., "Beam Seas Tests of Two Different Ship Models in Large Amplitude Regular Waves," Proceedings 9th International Conference on Stability of Ships and Ocean Vehicles, 2006.
3. Olivieri, A., Campana, E., Stern, F., and Francescutto, A., "Capsize High-Quality Data for Validation of URANS Codes," Proc. 26th ONR Symposium on Naval Hydrodynamics, Rome, Italy, 2006.
4. Olivieri, A., Francescutto, A., Campana, E., and Stern, F., "Parametric Roll Highly Controlled Experiments for an innovative ship design," 27th International Conference on Offshore Mechanics and Arctic Engineering, Estoril, Portugal 15-20 June 2008**.**
5. Carrica, P.M., Wilson, R.V., and Stern, F., "An Unsteady Single-Phase Level Set Method for Viscous Free Surface Flows," International Journal Numerical Methods Fluids, Vol. 53, Issue 2, 20 January 2007, pp. 229-256.
6. Carrica, P., Wilson, R., Noack, R., and Stern, F., "Ship Motions using Single-Phase Level Set with Dynamic Overset Grids, Computers & Fluids, Vol. 36, 2007, pp. 1415-1433.
7. Xing, T., Carrica, P., and Stern, F., "Computational Towing Tank Procedures for Single Run Curves of Resistance and Propulsion," ASME J. Fluids Eng, submitted 22 January 2008.
8. Umeda, N., Hashimoto, H., Vassalos, D, Urano, S. and Okou, K. "Nonlinear Dynamics on Parametric Roll Resonance with Realistic Numerical Modeling", International Shipbuilding Progress, Vol. 51, No 2/3, 2004, pp. 205-220.
9. Hashimoto, H., Umeda, N. "Nonlinear Analysis of Parametric Rolling in Longitudinal and Quartering seas with Realistic Modeling of Roll-Restoring Moment", Journal of Marine Science and Technology, vol.9, No.3, 2004, pp.117-126.
10. Noack R. 2005 SUGGAR: a General Capability for Moving Body Overset Grid Assembly, AIAA paper 2005-5117, *17th AIAA Computational Fluid Dynamics Conference*, Toronto, Ontario, Canada.
11. Boger DA, Dreyer JJ. Prediction of Hydrodynamic Forces and Moments for Underwater Vehicles Using Overset Grids. AIAA paper 2006-1148, 44th AIAA Aerospace Sciences Meeting, Reno, Nevada, 2006.
12. Himeno, Y. 1981 Prediction of Ship Roll Damping – State of the Art, University of Michigan, Report No. 239.
13. Irvine, M., Longo, J., Stern, F., "Towing Tank Tests for Surface Combatant for Free Roll Decay and Coupled Pitch and Heave Motions," Proc. 25th ONR Symposium on Naval Hydrodynamics, St Johns, Canada, 2004.
14. Bulian, G., Francescutto, A., "Theoretical prediction and experimental verification of multiple steady states for parametric roll", Accepted for presentation at 10th International Workshop on Ship Stability and Operational Safety, Daejeon, March 2008.

Table 1: Principal dimensions of the ONR Tumblehome and 5415/5512

	ONR Tumblehome								5415/5512
	EFD W/O BKs			CFD W/O BKs				CFD & EFD W/ BKs	EFD W/O BKs
L_{PP}	3.305 m			3.305 m				3.305 m	3.048 m
Draft (T)	0.1201 m			0.118 m				0.118 m	0.132 m
Beam (B_{WL})	0.403 m			0.403 m				0.403 m	0.405 m
Displ.	84.7 kg			84.7 kg				84.7 kg	86.4 kg
LC_G	1.708 m Aft of FP			1.708 m Aft of FP				1.708 m Aft of FP	1.536 m Aft of FP
KG	0.175	0.170	0.165 m	0.175	0.170	0.165	0.160 m	0.165 m	0.162 m
GM	0.033	0.038	0.043 m	0.033	0.038	0.043	0.048 m	0.043 m	0.043 m
k_{XX}	0.146 0.127	0.146 0.125	0.146 m 0.123 m	0.1388	0.153 0.1246	0.153 0.1298	0.153 m	0.153 m=38% B_{WL}	0.158 m=38% B_{WL}
$k_{YY} = k_{ZZ}$	0.826 m =25% LPP 0.737 m =22% LPP			0.826 m =25% LPP				0.826 m =25% LPP	0.762 m=25% LPP
BKs								c = 26.82 mm L = 1098 mm	

Table 2: Summary of 2DOF zero-speed heave-roll in beam waves results for Ak=0.156

	EFD			CFD			E % D		
	1st order Amplitude a_1	2nd order Amplitude a_2	a_2/a_1	1st order Amplitude a_1	2nd order Amplitude a_2	a_2/a_1	1st order Amplitude	2nd order Amplitude	Phase Error for domnant harmonic deg
Z/A	1.07	0.079	0.07	1.22	0.060	0.05	-14.02	24.05	3.08
ϕ/ak	2.90	0.221	0.08	1.66	0.125	0.07	42.76	43.44	6.11
X	1.71E-3	3.84E-3	2.25	5.56E-4	3.91E-4	0.70	67.48	89.82	24.13
Y	0.067	3.54E-3	0.05	0.053	5.41E-3	0.10	20.89	-52.82	5.12
M	2.36E-4	4.00E-4	1.69	1.10E-4	1.74E-4	1.58	53.39	56.50	-24.61
N	5.89E-4	7.82E-5	0.13	7.29E-4	1.42E-4	0.19	-23.77	-81.58	17.42

Table 3: Summary of 3DOF forward-speed heave-roll-pitch in head waves results

	EFD Ak=0.115			CFD Ak=0.115 Ak=0.156			E % D Ak=0.115		
	1st order Amplitude a_1	2nd order Amplitude a_2	a_2/a_1	1st order Amplitude a_1	2nd order Amplitude a_2	a_2/a_1	1st order Amplitude	2nd order Amplitude	Phase Error for domnant harmonic deg
Z/A	0.860	0.053	0.06	0.876 0.780	0.0397 0.041	0.04 0.05	-1.92	25.00	4.02
θ/ak	0.446	0.028	0.06	0.401 0.374	0.027 0.030	0.07 0.08	10.20	5.91	4.81
X	8.74E-3	4.28E-3	0.49	4.16E-3 4.79E-3	4.20E-3 5.79E-3	1.01 1.21	52.36	1.93	5.57

Table 4: CFD & EFD estimates for GM_m, GM_a, and frequencies

	GM=0.033						GM=0.038						GM=0.043					
Method	kxx	GM_m	GM_a	$\omega_{\phi h}$	ω_ϕ	ω_a	kxx	GM_m	GM_a	$\omega_{\phi h}$	ω_ϕ	ω_a	kxx	GM_m	GM_a	$\omega_{\phi h}$	ω_ϕ	ω_a
CFD	0.1388	0.019	0.027	4.099	3.110	3.708	0.153 0.1246	0.024 0.024	0.026 0.026	3.99 4.90	3.17 3.89	3.300 4.053	0.153 0.1298	0.0283 0.0283	0.025 0.025	4.24 5.00	3.44 4.06	3.237 3.815
EFD (OU)	0.1388	0.028	0.012	4.099	3.776	2.472	0.1388	0.0329	0.012	4.39	4.09	2.472	0.1388	0.038	0.012	4.67	4.40	2.472

Table 5: Parametric rolling zone and max roll angle predicted by CFD, EFD, NDA, and Mathieu Equation

Method	GM=0.033 m				GM=0.038 m				GM=0.043 m				GM=0.048 m			
	kxx	FR range Min	FR range Max	Max roll (deg)	kxx	FR range Min	FR range Max	Max roll (deg)	kxx	FR range Min	FR range Max	Max roll (deg)	kxx	FR range Min	FR range Max	Max roll (deg)
CFD	0.1388	0.0	0.3	50	0.153 0.1246	0.17 0.18	0.44	capsize 45	0.153 0.1298	0.1 No PR	0.35	37 -	0.153	0.11	0.35	60
EFD	0.127	0.07	0.28	40	0.125	0.18	0.35	35	0.123	No PR		-	N/A	N/A		N/A
NDA:Poincare(i) Poincare' (d)	0.1388	0.11	0.34	20	0.1388 (i) (d)	0.195 0.13	0.38 0.38	30	0.1388	No PR		-	N/A	N/A		N/A
NDA: Average	0.1388	0.225	0.34	22.5	0.1388	0.28	0.38	28	0.1388	0.325	0.35	29	N/A	N/A		N/A
Mathieu Eq.	0.1388	0.0	0.26	∞	0.1246	0.07	0.41	∞	0.1298	0.07	0.41	∞	0.153	0.0	0.32	∞

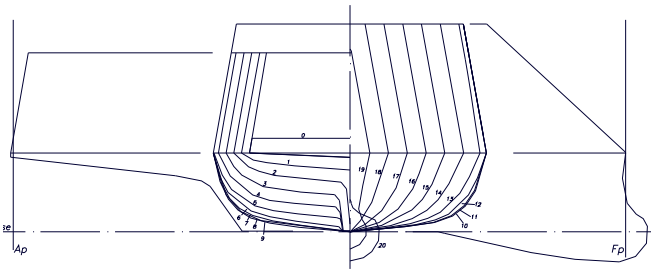

Figure 1: ONR Tumblehome body-plan and center contour line

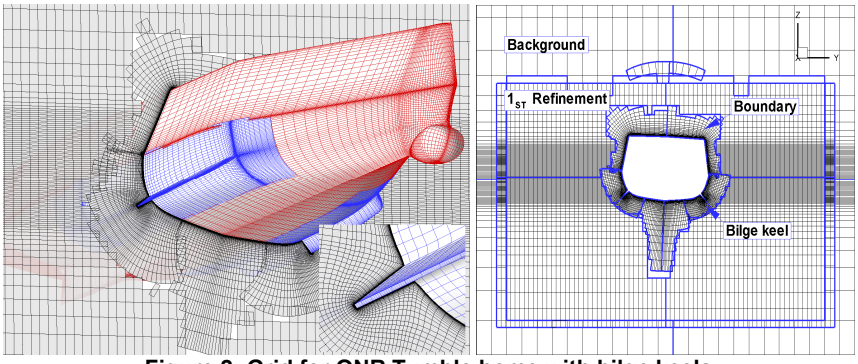

Figure 2: Grid for ONR Tumble home with bilge keels

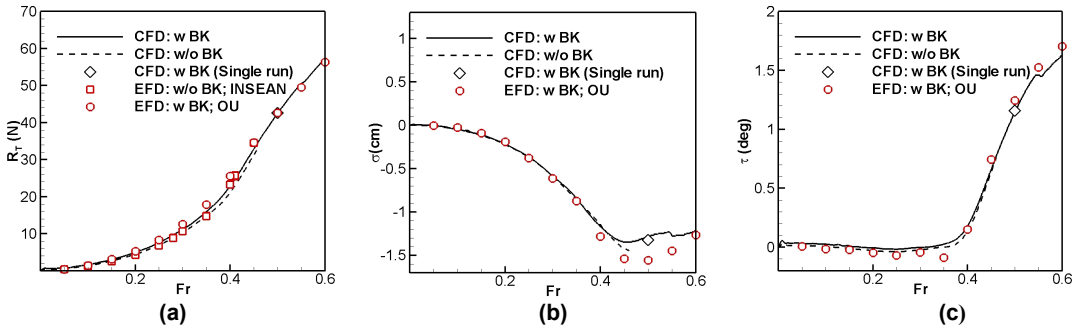

Figure 3: Calm water results: (a) resistance, (b) sinkage, (c) trim versus Fr number

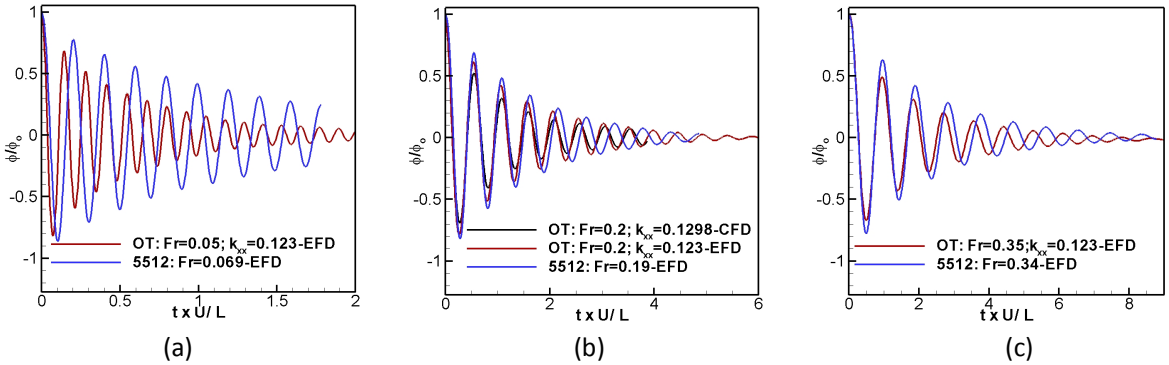

Figure 4: Roll decay for OT and 5512 for design GM (OT:ϕ_0=25 deg; 5512:ϕ_0=20 deg): (a) Low Fr; (b) Medium Fr (c) High Fr

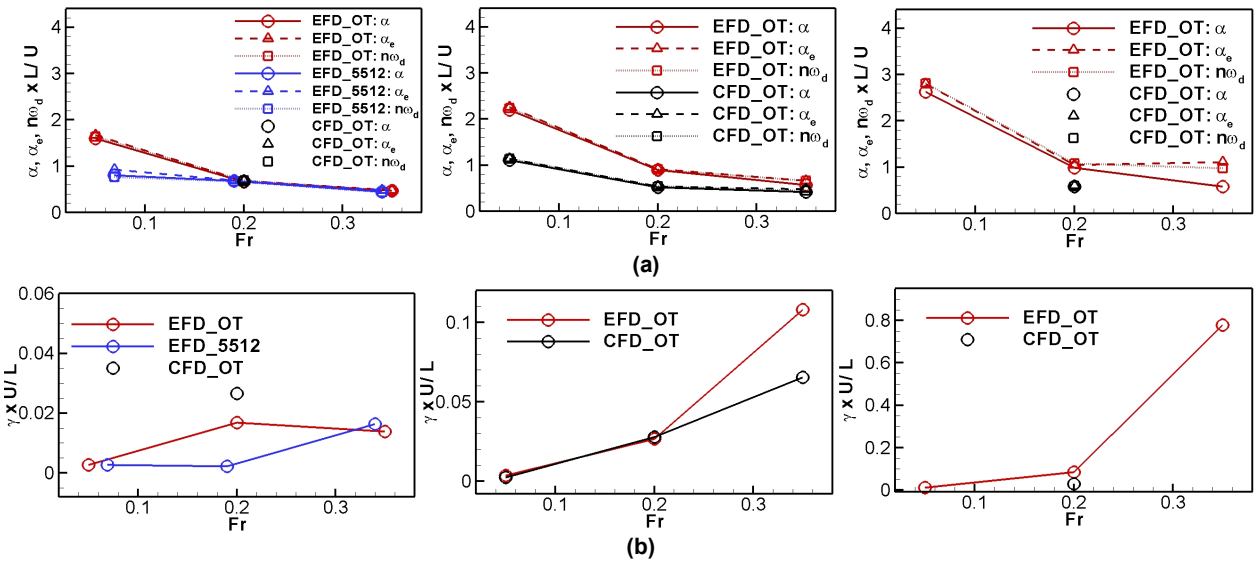

Figure 5: CFD and EFD damping coefficients for OT and 5512: (a) linear for GM=0.043 (left), GM=0.038 (middle), and GM=0.033 (right), (b) cubic for GM=0.043 (left), GM=0.038 (middle), and GM=0.033 (right)

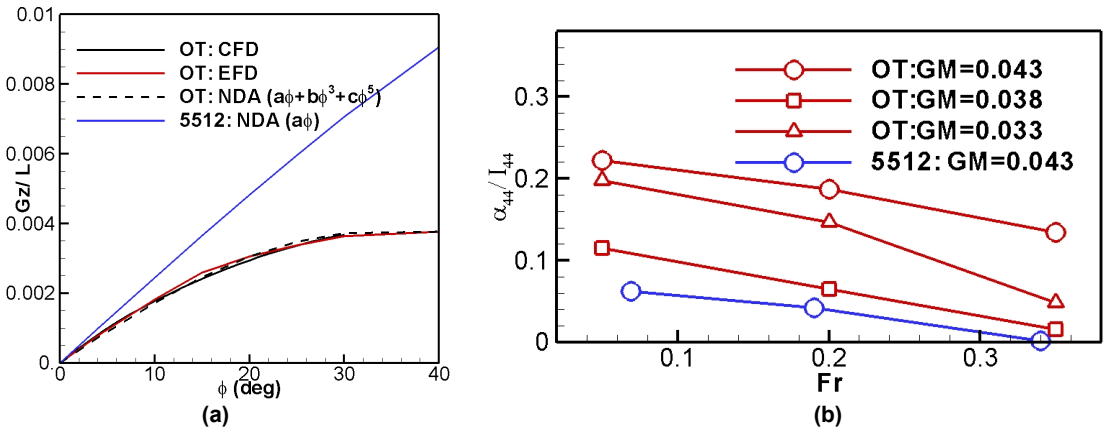

Figure 6: OT and 5512 comparison: (a) Non-dimensional GZ curve for design GM; (b)added mass

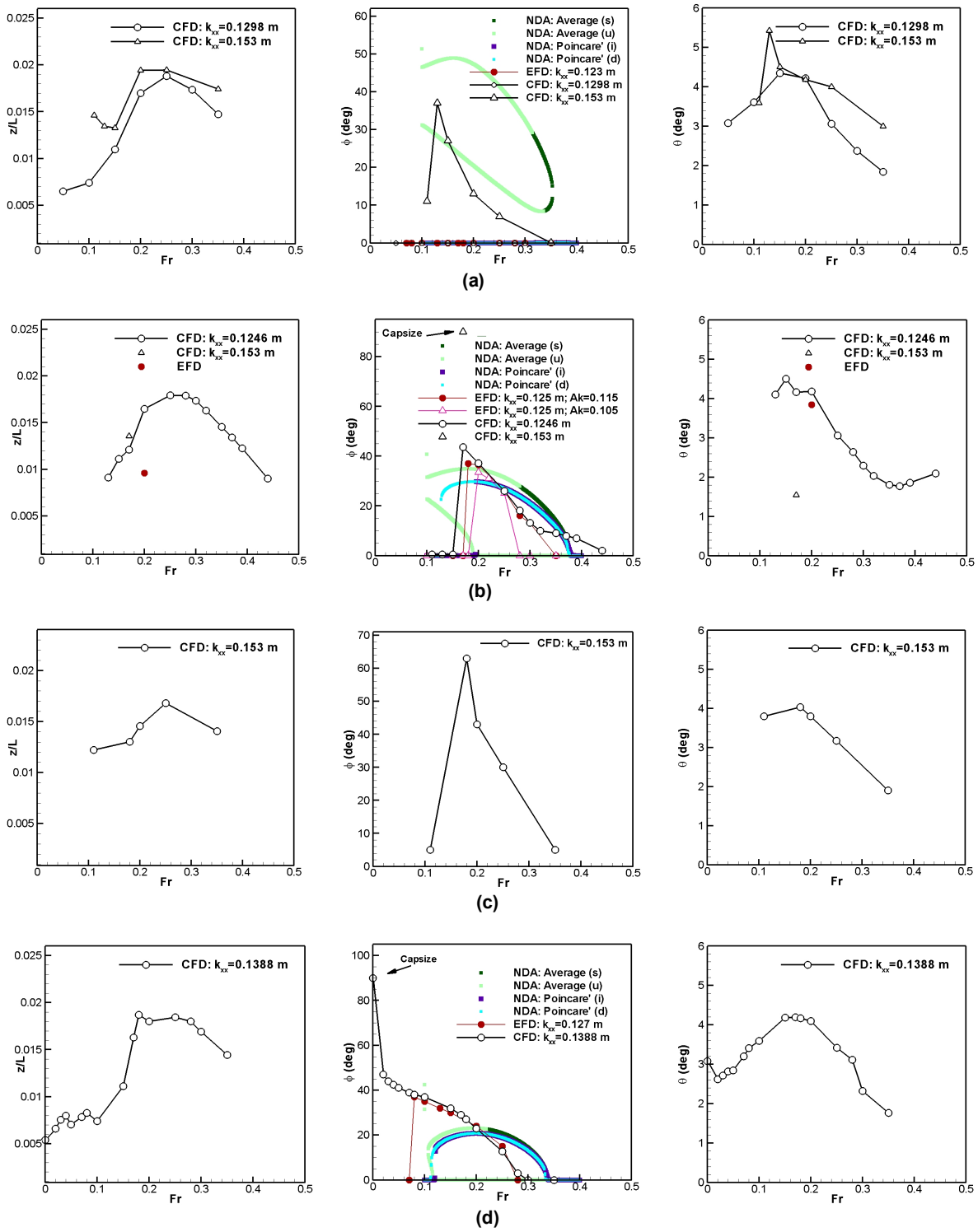

Figure 7: Parametric rolling motions for all GM: (a) Gm=0.043 m, (b) Gm=0.038 m, (c) GM=0.048 m, (d) GM=0.033 m

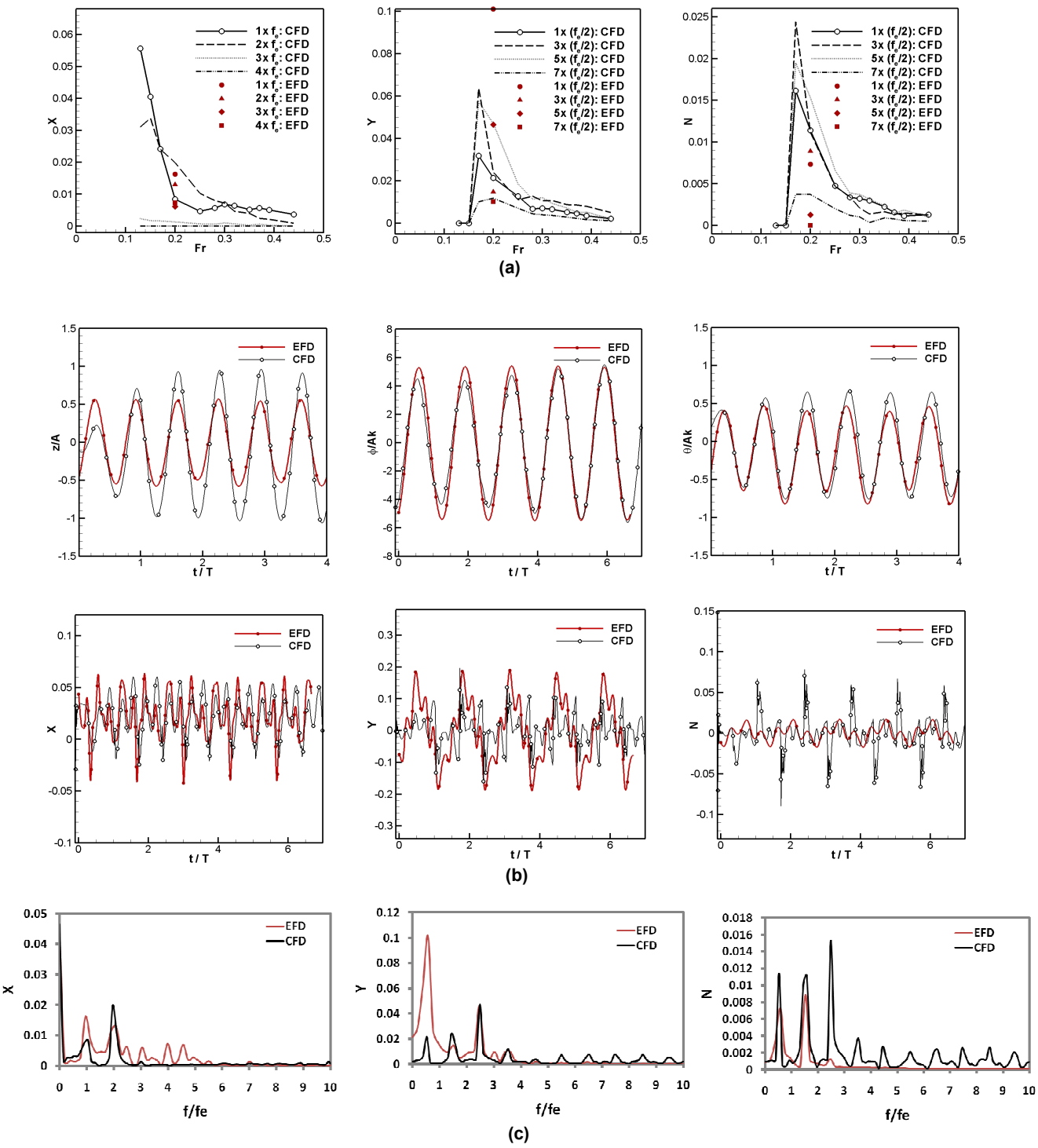

Figure 8: Parametric rolling results for GM=0.038 m: (a) dominant harmonics of CFD (kxx=0.1246) and EFD forces and moments, (b) CFD (kxx=0.1246) and EFD time history comparison for Fr=0.2, (c) CFD (kxx=0.1246) and EFD FFT comparison for Fr=0.2